HYDROLOGICAL PROCESSES
Hydrol. Process. (2016)
Published online in Wiley Online Library
(wileyonlinelibrary.com) DOI: 10.1002/hyp.10884

Vertical surface water–groundwater exchange processes within a headwater floodplain induced by experimental floods

Erich T. Hester,* Christopher R. Guth,[1] Durelle T. Scott[2] and Charles N. Jones[2]
[1] *The Charles E. Via, Jr. Department of Civil and Environmental Engineering, Virginia Tech, 220-D Patton Hall, Blacksburg, VA, 24061, USA*
[2] *Department of Biological Systems Engineering, Virginia Tech, 305 Seitz Hall, Blacksburg, VA, 24061, USA*

Abstract:

Restoring hydrologic connectivity between channels and floodplains is common practice in stream and river restoration. Floodplain hydrology and hydrogeology impact stream hydraulics, ecology, biogeochemical processing, and pollutant removal, yet rigorous field evaluations of surface water–groundwater exchange within floodplains during overbank floods are rare. We conducted five sets of experimental floods to mimic floodplain reconnection by pumping stream water onto an existing floodplain swale. Floods were conducted throughout the year to capture seasonal variation and each involved two replicate floods on successive days to test the effect of varying antecedent moisture. Water levels and specific conductance were measured in surface water, soil, and groundwater within the floodplain, along with surface flow into and out of the floodplain. Vegetation density varied seasonally and controlled the volume of surface water storage on the floodplain. By contrast, antecedent moisture conditions controlled storage of water in floodplain soils, with drier antecedent moisture conditions leading to increased subsurface storage and slower flood wave propagation across the floodplain surface. The site experienced spatial heterogeneity in vertical connectivity between surface water and groundwater across the floodplain surface, where propagation of hydrostatic pressure, preferential flow, and bulk Darcy flow were all mechanisms that may have occurred during the five floods. Vertical connectivity also increased with time, suggesting higher frequency of floodplain inundation may increase surface water–groundwater exchange across the floodplain surface. Understanding the variability of floodplain impacts on water quality noted in the literature likely requires better accounting for seasonal variations in floodplain vegetation and antecedent moisture as well as heterogeneous exchange flow mechanisms.

KEY WORDS hyporheic exchange; floodplain connectivity; riparian zone; overbank flooding hydraulics; preferential flow; stream restoration

Received 29 October 2014; Accepted 11 April 2016

INTRODUCTION

Natural floodplain functioning

Floodplain connectivity is described as the exchange of matter and energy between a stream channel and its floodplain which can benefit water quality and ecosystem health (Ward, 1997; Pringle, 2003). When coupled with natural variability in storm magnitude and inundation frequency, floodplain connectivity can directly influence ecosystem function (Junk *et al*., 1989; Poff *et al*., 1997; Tockner *et al*., 2000; Knispel *et al*., 2006; Langhans and Tockner, 2006) by connecting landscape patches and biological processes occurring at various spatial and temporal scales (Amoros and Bornette, 2002). During overbank floods, surface water velocities decrease in floodplains relative to the channel, resulting in increased potential for reactions, such as net production or removal of nutrients (Bukaveckas, 2007; Kronvang *et al*., 2007; Harrison *et al*., 2014). Floodplain topography dictates surface water storage and mixing on the floodplain (Mertes, 1997) and floodplain soil properties affect surface water and groundwater flow and exchange across the floodplain surface (Krause and Bronstert, 2007; Doble *et al*., 2012; Helton *et al*., 2014).

Floodplain soils are often conceptualized as homogeneous (Bates *et al*., 2000; Krause *et al*., 2007; Welch *et al*., 2013), yet recent studies show heterogeneity and preferential flow often control transport (Fox *et al*., 2006; Fuchs *et al*., 2009; Heeren *et al*., 2014; Menichino *et al*., 2014). Groundwater recharge during overbank flood events has been evaluated in a variety of floodplain environments (Dahan *et al*., 2008; Doble *et al*., 2011a; Doble *et al*., 2012). The rate at which surface water infiltrates into the floodplain subsurface can be heavily affected by low hydraulic conductivity (K) sediments (Jolly *et al*., 1994; Andersen, 2004; Doble *et al*., 2011b) and local ponding on the floodplain surface (Jung *et al*., 2004).

*Correspondence to: Erich T. Hester, The Charles E. Via, Jr. Department of Civil and Environmental Engineering, Virginia Tech, 220-D Patton Hall, Blacksburg, VA 24061, USA.
E-mail: ehester@vt.edu

The presence of paleochannels (Stanford and Ward, 1993; Poole *et al.*, 2002) and preferential flow paths (Bramley *et al.*, 2003; Heeren *et al.*, 2010) can increase average infiltration rates. This in turn can reduce residence times and contact with floodplain sediments, reducing the potential for nutrient removal (Nieber, 2000; Fuchs *et al.*, 2009; Heeren *et al.*, 2010).

During overbank floods, surface water can enter the floodplain vertically across the floodplain surface or laterally across the channel banks, with the later process referred to as bank storage or 'lung model' hyporheic exchange (Pinder and Sauer, 1971; Sawyer *et al.*, 2009). All such exchange flow between channel and floodplain groundwater can occur by Darcy flow and potentially non-Darcy flow (Menichino *et al.*, 2014; Menichino and Hester, 2015). Floodplain groundwater levels can also increase in response to elevated stream stage with a response time too quick to be explained by Darcy or non-Darcy flow (Käser *et al.*, 2009; Vidon, 2012). These pressure waves (or kinematic waves) are commonly observed but not well understood (Singh, 2002). Developing a mechanistic understanding of groundwater dynamics within the floodplain will ultimately lead to a more holistic understanding of floodplain hydraulics, ecology, and biogeochemistry, including interaction with the channel.

Human impacts and restoration

Human induced land cover change and river regulation have altered the natural flow regime in many streams and rivers, decreasing the ecosystem services provided by the river network (Poff *et al.*, 1997). Urbanization has reduced evapotranspiration and infiltration, increased peak discharges, and lowered baseflow in many areas (Leopold, 1968; Lerner, 2002; O'Driscoll *et al.*, 2010). Larger peak discharges in turn enhance the sediment carrying capacity of streams (Lane, 1955), often resulting in increased channel incision (Graf, 1975; Booth, 1990; Doll *et al.*, 2002). In addition, legacy sediments from centuries of agricultural practices have raised many floodplain surfaces through depositional processes (Walter and Merritts, 2008). From a network perspective, these combined effects have led to the reduction of floodplain connectivity and its associated benefits (Craig *et al.*, 2008).

Stream restoration is a common technique that attempts to mitigate functional loss in streams (Wohl *et al.*, 2005; Hester and Gooseff, 2010; Landers, 2010; Simon *et al.*, 2011). The most common stream restoration goals in the United States are improving aquatic habitat, increasing bank stability, and improving water quality (Bernhardt *et al.*, 2005). Recently, the restoration industry has recognized the importance of lateral connectivity and floodplain reconnection has become a common practice (Boon, 1998; Harrison *et al.*, 2014). Yet understanding the hydraulic, ecological, and water quality effects of floodplain restoration or reconnection requires understanding floodplain hydraulics, including surface water–groundwater exchange across the floodplain surface during overbank events.

Objectives

The overall objective of this study was to conduct inundation experiments in a floodplain typical of a headwater stream, and do so over a range of seasons and antecedent soil moisture conditions. During these experimental floods we sought to characterize surface water flow on the floodplain and vertical surface water–groundwater exchange across the floodplain surface. Our aim was to replicate natural conditions typical of an overbank flood event as much as possible while maintaining control over flood timing and discharge, as well as characterization of vertical exchange mechanisms across the floodplain surface at greater spatial and temporal resolution than is typical of previous studies.

We sought to answer a series of fundamental questions about how overbank floods function in this setting, including (1) How does the volume of water that is (a) stored on the floodplain surface and (b) exchanged vertically across the floodplain surface (i.e. enters floodplain groundwater) during floods vary with season and antecedent moisture conditions?, (2) Are the rates and mechanisms of surface water–groundwater exchange across the floodplain spatially and temporally variable?, and (3) Is surface water–groundwater exchange across the floodplain surface generally slow and consistent with Darcy flow through the fine grained soils comprising the floodplains or is there evidence of preferential flow bypassing the matrix? Lateral exchange across the banks (i.e. bank storage) was not explicitly addressed, but we do discuss our results in that broader context.

METHODS

Site description

The study site is along a floodplain reach of Stroubles Creek, a third-order alluvial stream near Blacksburg, Virginia, with average discharge of $0.22\,m^3/s$ and approximate bankfull depth of 0.7 m. The catchment area is approximately $15\,km^2$ and is predominantly urban (84%). Agricultural land (13%) and forest (3%) are also present. The site is within the Stream Research, Education, and Management Lab (StREAM Lab, www.bse.vt.edu/site/streamlab), an extensively monitored reach of Stroubles Creek. Reed canary grass, a nonnative grass, is prevalent throughout the floodplain. Stream restoration activities including cattle exclusion, cutting back over-steepened banks, and construction of inset floodplains have occurred along the channel within the past decade. We chose this site because it has extensive stream and hydrologic monitoring as part of the StREAM Lab and is typical of stream restoration projects in the US Mid-Atlantic Region in terms of stream size and land use.

Field methods

Experimental floods and water budget. We conducted a series of five experimental overbank flood events over the course of a year (Table I). The series of floods accounted for seasonal variation in evapotranspiration rates, soil moisture, vegetation density, baseflow, and groundwater elevations. For each experimental flood we pumped surface water from Stroubles Creek for 3 h into a small floodplain depression or swale that appeared to be an abandoned oxbow (Figure 1). During the second hour of each flood a pulse of NaCl and $NaNO_3^-$ was injected into the pumped water. This injection was part of a separate study focused on biogeochemical transformations in the floodplain surface water (Jones *et al.*, 2015) and is mentioned here because the injection affected our results in minor, but observable, ways (see Results and Discussion sections). In order to quantify the effect of antecedent moisture conditions on the hydraulics, separate floods occurred on two or more consecutive days. When possible, the first day of pumping for each flood was preceded by at least two days with no precipitation to ensure that the observed hydraulic responses were a result of the experimental flood rather than a natural rainfall event. The second flood then occurred with wet conditions, allowing comparison to the drier first flood. These experimental floods mimicked natural overbank floods in many respects, but also deviated from natural conditions in some ways, such as greater frequency (see section on Limitations of study). We also continuously monitored background conditions between experimental floods (Figures 4, 5).

We used a Berkeley B3-ZRMS pump to inundate the floodplain. Pump flow rates were measured using a Fuji M-flow meter during the Spring, Early Summer, Late Summer, and Fall floods. Because of malfunction of the Fuji M-Flow meter, we used a Sensus 1125-W fire hydrant flow meter during the Winter flood. Flow rates entering the site averaged 23.9 L s^{-1} across all five floods, with a standard deviation of 1.6 L s^{-1} (Table I). In order to more accurately represent natural flow conditions, water velocities were reduced first through a large corrugated 23-cm-diameter irrigation pipe and then a series of cinder blocks on a tarp.

We measured the discharge rate of surface water leaving the flood site using a 7.62-cm fibreglass Parshall flume (Engineered Fiberglass Composites, Inc.) installed at the downstream end of the swale (Figure 1). We used plywood to taper flow into the flume and inserted the built-in flange approximately 20 cm into the ground to reduce flow bypassing the flume through groundwater. Leaks between the flume, plywood, and ground were sealed using a combination of aluminium sheeting, duct

Table I. Experimental floods

Flood event	Dates of flooding	Times of flooding	Average pump flow rate (L s^{-1})	Antecedent groundwater elevation, XS1-Centre-30 cm (cm above 600 m elevation)[c]	Antecedent soil moisture, XS1-5 cm (% Sat)[c]	Evapotranspiration rate, first day (mm d^{-1})[d]
Spring	April 8, 2013	12:18–3:18 PM	23.4	60	99.2	2.85
	April 9, 2013	12:01–3:01 PM	23.4[b]	60	98.9	
Early summer	June 29, 2013	9:42 AM–12:42 PM	21.8	60	91.2	4.10
	June 30, 2013	9:42 AM–1:06 PM[a]	21.6	61	90.8	
	July 1, 2013	9:13 AM–12:13 PM	21.8[b]	62	90.2	
Late summer	August 30, 2013	12:15–3:15 PM	24.6	6	89.7	3.59
	August 31, 2013	12:00 –3:00 PM	24.6[b]	59	95.8	
Fall	November 11, 2013	1:01–3:01 PM	26.4	9	80.5	2.11
	November 12, 2013	1:39–4:49 PM	25.4	58	96.5	
Winter	February 7, 2014	1:14–4:14 PM	23.3	62	97.2	0.82
	February 8, 2014	12:50–3:50 PM	22.5	61	97.3	

[a] The pump piping system became detached and required the pump to be turned off briefly. Three total hours of pumping surface water onto the floodplain were completed, although this time was not continuous and instead occurred off-and-on over the timeframe listed. This interruption in inflow resulted in the need for a third day of flooding to be completed.
[b] Flow meter malfunctioned on second day and flows from first day are given.
[c] Groundwater levels and soil moisture levels are for single locations at the XS1 transect. Other locations have different values (generally greater fluctuations in moisture levels because XS1 is the wettest location in the swale), but would exhibit drying and wetting trends at similar times (see Figures 4 and 5).
[d] Hourly evapotranspiration rates were estimated as part of a separate study using a standard Bowen Ratio approach based on data from a weather station 80 m distant from the flood site (solar radiation, air temperature, relative humidity, barometric pressure, rainfall, soil moisture) and are summed here for the first day of each experimental flood—see (Jones *et al.*, 2015) for detailed methods.

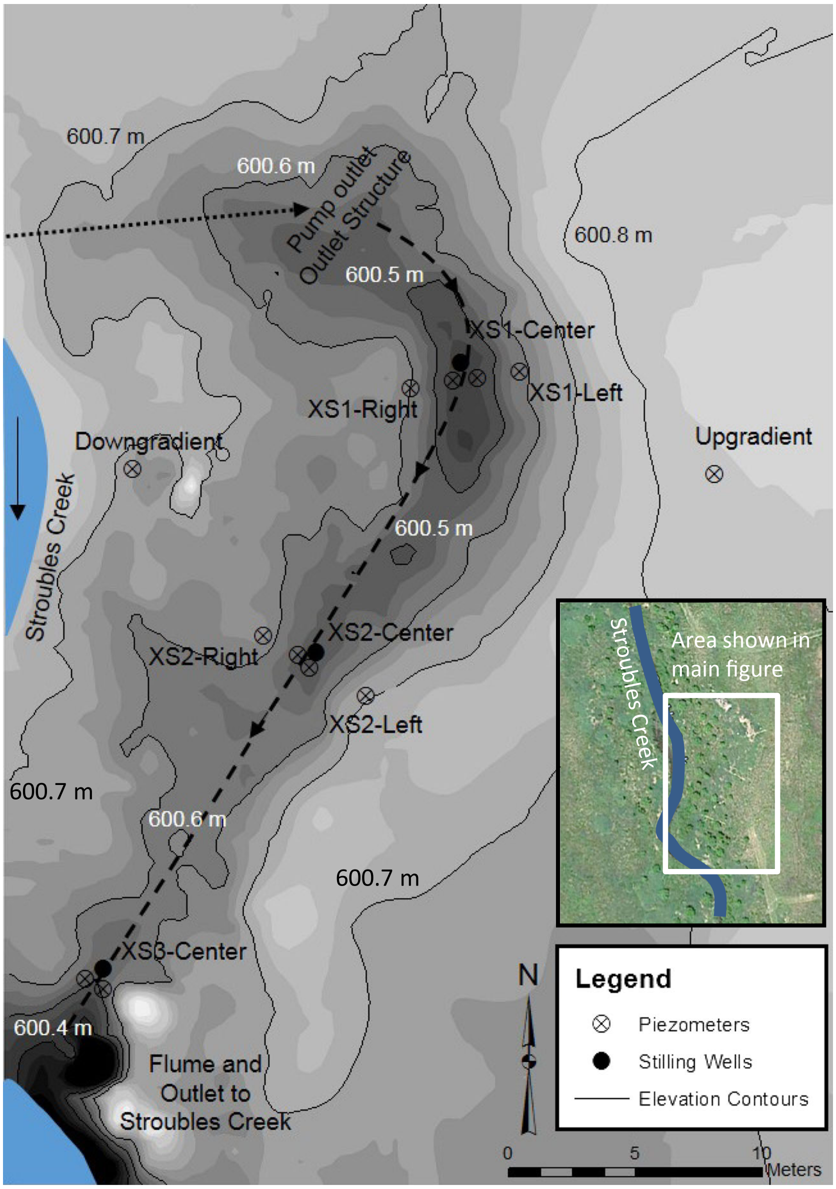

Figure 1. Map of study site. Dotted line shows pipe from Stroubles Creek to swale and dashed line shows approximate flood centreline. Double piezometers at the Centre locations (XS1-Centre, XS2-Centre, XS3-Centre) indicate nested piezometers (shallow at ~30 cm BGS and deep at ~100 cm BGS). Piezometer to Left and Right of Centre at XS1 and XS2 are shallow (~30 cm). Upgradient and Downgradient piezometers are deep (~100 cm). Soil moisture probe locations are not shown separately, but are co-located with the piezometers at XS1-Left, XS1-Centre, XS1-Right, XS2-Left, XS2-Centre, XS2-Right, and XS3-Centre. Elevation contours are for land surface topography with a 0.1-m interval. BGS = (depth) below ground surface

tape, marine epoxy, and sand bags. We installed an Onset HOBO Pressure Transducer to measure the water column depth in the flume.

Surface and groundwater hydraulics and electrical conductance. We monitored groundwater with polyvinyl chloride (PVC) piezometers with an internal diameter of 3.81 cm and single 10 cm screened interval covered by nylon mesh filter fabric attached with electrical tape. Piezometer bottoms were capped but had small holes to allow drainage. We monitored surface water with stilling wells that were similar to the piezometers, but no filter fabric was used and the screened length was much greater.

Piezometers were inserted into bore holes created with a 3.8-cm-diameter hand auger bit. We placed the piezometers in three transects centred along the estimated centreline of surface flow through the swale (Figure 1). We placed piezometer screens at two depths: shallow at ~30 cm below ground surface (BGS) typically in a shallow clay layer, and deep ~100 cm BGS typically below the clay in a layer of gravel mixed with silts. We used boreholes with diameters similar to that of the piezometers in order to minimize the potential for short circuiting of surface water into the subsurface and to reduce the impact on the natural floodplain soil structure. This prevented the need for filter sand backfill because of continuous contact between the piezometer and the surrounding natural soils. Nevertheless, we packed the piezometer–soil interface at the surface with bentonite as extra protection against artificial connection between surface water and the subsurface.

We installed piezometers in nested pairs (30 cm and 100 cm BGS) at the centreline location of each transect, while only shallow piezometers (30 cm BGS) were placed to the left and right of the centreline (Figure 1). We used only one monitoring location at cross section 3 (XS3-Centre in Figure 1) because of convergence of surface flow near that location. We installed one deep piezometer (100 cm BGS) further back in the floodplain away from Stroubles Creek ('Upgradient' in Figure 1) and conversely one 'Downgradient' near the creek to measure larger scale groundwater hydraulic head and electrical conductivity gradients that put the flood experiment results in context. We routinely repacked bentonite next to the piezometers throughout the study duration to prevent preferential flow paths (PFPs) from forming artificially down the piezometer bore holes. We classified soils from borehole cores along the site centreline during the installation of the deep piezometers. Soils were classified as organic, clay, or sand/gravel using both visual and textural characteristics. Classification of gravel sediments was clear because of its coarse nature. Clay and organic soil layers were distinguished from each other through the analysis of ribbon lengths using the screening-level 'feel method' (Thien, 1979). This is a qualitative but standard approach that can reliably distinguish soil texture classes (Arshad *et al*., 1996). Last, we installed stilling wells on the floodplain surface at each of the three cross section centreline locations to measure surface water properties.

We installed a variety of instruments to measure pressure (water level), soil moisture, and electrical conductivity in surface water, groundwater, and soil. We installed 11 Solinst LTC Levellogger Junior 3001 sensor/loggers to measure pressure and electrical conductivity in the surface water stilling wells at XS1-Centre and XS2-Centre, in each of the centreline nested piezometers (shallow and deep at XS1-Centre, XS2-Centre, and XS3-Centre), in the Upgradient piezometer, and in piezometers XS2-Left and XS2-Right (Figure 1). We also installed 6 Onset HOBO sensor/loggers to measure pressure in the air, in the Parshall flume stilling well, in the surface water stilling well at XS3-Centre, in piezometers XS1-Left and XS1-Right, and in the Downgradient piezometer near Stroubles Creek (Figure 1). We measured soil moisture content in shallow soils (5 cm BGS and 10 cm BGS) adjacent to each piezometer in the flooded area. We placed Decagon Devices GS3 soil moisture probes which measure volumetric moisture content and electrical conductivity along the centreline (6 probes total) and Decagon Devices 5TM soil moisture probes which measure volumetric moisture content at the other four locations (8 probes total). We used Campbell Scientific CR200 loggers to store data during probe deployment. Beginning with the Early Summer flood, the LTC located at XS2-Left was switched with the HOBO located at XS3-Centre-Surface. All other instrumentation was kept constant between flood events. We identify instrument locations based on the transect in which they were installed (i.e. XS1, XS2, or XS3), their location relative to the flow centreline (i.e. Left, Centre, or Right), and their measurement depth (e.g. surface, 30 cm BGS, etc.). For example, the piezometer located to the left of the flow centreline at XS1 at a depth of 30 cm BGS is identified as XS1-Left-30 cm.

Logging frequencies for the LTCs and HOBOs evolved somewhat during the year as we refined our approach. During the Spring flood we set logging frequencies for the LTCs and HOBOs measuring surface water properties to 5 min while the subsurface instruments recorded data every 15 min. All soil moisture probes were also set at a logging interval of 5 min. Water depth in the flume was recorded every 2 min during the Spring flood. Logging intervals for the Early Summer flood were identical to Spring except that the flume logging interval was reduced to every minute. The logging interval for all LTCs and HOBOs (surface, subsurface, and Parshall flume) was set at 2 min for the Late Summer, Fall, and Winter floods. We kept all instrumentation installed on the flood site between flood events with a logging interval of 15 min. We obtained hourly precipitation data from a weather station located approximately 80 m to the north of the swale that is part of the Virginia Tech StREAM Lab (streamlab.bse.vt.edu).

We conducted rising head (bail) tests to measure K of soil near each piezometer (Landon *et al*., 2001). We did this near the beginning (June 12, 2013) and end (March 8, 2014) of the study to track changes in K. We used instrumentation already in each piezometer but reset the logging interval to 15 s. We extracted water from each piezometer using a Geotech peristaltic pump. We changed logging frequencies back to 15-min intervals approximately 48 h after the start of the rising head test. Piezometers in very low K soils (XS2-Right, XS3-Centre-30 cm, XS3-Centre-100 cm, Upgradient, Downgradient) had not returned to background levels by this time during the June 2013 tests.

Data analysis

We calculated a series of metrics to quantify the amount of water stored in the floodplain as a result of the experimental floods. We defined the total volumetric storage of flood water as the sum of the surface and subsurface storage volumes

$$
\begin{aligned}
V_{total\ storage} &= V_{surface\ storage} + V_{subsurface\ storage} \\
&= V_{pumped} - V_{out} - V_{error}
\end{aligned} \tag{1}
$$

where $V_{total\ storage}$ (L^3) is calculated as the volume of water experimentally applied to the site (V_{pumped}, L^3) minus that leaving through the flume (V_{out}, L^3) from the time the pump was turned on until the time when flow through the flume ceased, minus an error term (V_{error}, L^3) because of leakage around the flume during that time. Equation 1 was evaluated for the first day of flooding, because storage was generally larger and more variable on the first day because of drier conditions in some seasons. We also calculated the volume of water that drained from the site after each flood ($V_{drained}$, L^3) by integrating the flume flow rate from when the pump was turned off to when flow through the flume stopped. We conducted this analysis for the second day of flooding for each season because antecedent soil moisture and water levels were similar for each season. Observed differences could then be attributed to seasonal changes (e.g. vegetation) rather than differences in antecedent moisture. $V_{total\ storage}$ and $V_{drained}$ were then normalized to the total volume of surface water applied to the site (V_{pumped}) to account for variations in inflow discharge rates.

In addition, we calculated metrics to quantify the effect of the experimental floods on floodplain water levels. First, we calculated the observed maximum change in water levels in surface water and the four groundwater locations at each transect (30 cm at Left and Right, 30 cm and 100 cm at Centre) as a result of the flood ($\Delta H_{surface}$ and $\Delta H_{subsurface}$, respectively, L). We calculated these changes in water level as the flood peak (maximum water level within 24 h after start of the pump) minus the pre-event level. If another flood event started within the 24-h window, we used the maximum water level observed before the pump was turned on for the next flood. Next, we divided the water level change in groundwater by the water level change in the corresponding surface water measuring point (e.g. XS1 groundwater normalized to XS1 surface water), and averaged the four values for each transect (30 cm at Left and Right, 30 cm and 100 cm at Centre). We did this for XS1 and XS2 for both experimental flood days of each season, yielding four averaged values. This analysis was not completed for XS3 because of lack of groundwater response.

We also calculated vertical head gradients (I_z, L L^{-1}, with downward gradients positive in sign) along the flood centreline at each cross section using nested pairs of piezometers and stilling wells

$$
I_{zij} = \frac{H_j - H_i}{Z_j - Z_i} \tag{2}
$$

where H is the water level elevation (L, cm), Z is the elevation of the pressure sensor (i.e. screened inlet at 0, 30, or 100 cm BGS, L), and the subscripts i and j indicate successively deeper measurement locations, with Equation 2 evaluated for i,j pairs of 0 to 30 cm BGS, 0 to 100 cm BGS, and 30 to 100 cm BGS.

We also calculated a series of metrics to quantify the travel time of water within the floodplain. First, we calculated the flood arrival time or time needed for the flooding front to traverse the floodplain surface ($T_{surface}$, T) as the time from the flood start (turning on the pump) until water started flowing through the flume. Second, we calculated time for the flood signal to propagate from surface water vertically downward across the floodplain surface into groundwater. We calculated this as the difference in times when peak water levels occurred in surface water and groundwater, respectively ($T_{subsurface}$, T). Like for ΔH, we calculated this for each of the four groundwater locations (30 cm at Left and Right, 30 cm and 100 cm at Centre) at XS1 and XS2. We then averaged the values for the four locations at each transect for both floods, giving four averages (XS1 and XS2 for day 1 and day 2) for each season.

Finally, for comparison, we calculated theoretical, average, vertical, groundwater velocity (v, L T^{-1}) and Darcy travel time (T_{Darcy}, T) for the centreline piezometers

$$
v = \frac{KI_{max}}{n} \tag{3}
$$

$$
T_{Darcy} = \frac{d}{v} \tag{4}
$$

where K is the average hydraulic conductivity of the soil from the two rising head tests (June 2013 and March 2014, Table II) performed at each piezometer location (L T^{-1}), I_{max} is the maximum vertical head gradient observed throughout the course of the experimental flood between the surface water on the floodplain and the depth BGS of each piezometer (d, T), and n is the effective porosity of the soil which was assumed to be 0.3 ($L^3 L^{-3}$). Equation 4 estimates the vertical travel time if Darcy flow was the only mechanism by which the flood signal propagated into the subsurface. In Equation 3, we used the Hvorslev (1951) method to determine K

$$
K = \frac{r_c^2 \ln\left(\frac{L}{R}\right)}{2LT_o} \tag{5}
$$

where r_c is the piezometer radius (L), L is the screen length (L), R is radius of the screened portion of the piezometer

Table II. Hydraulic conductivity (K) results using the Hvorslev method

Location	K ($m\,s^{-1}$) Test 1 (12 Jun 2013)	Test 2 (8 Mar 2014)
XS1-Left-30 cm	3.8E − 07	ND
XS1-Centre-30 cm	3.2E − 06	6.08E − 06
XS1-Centre-100 cm	2.3E − 06	1.03E − 05
XS1-Right-30 cm	1.2E − 07	1.91E − 06
XS2-Left-30 cm	8.8E − 09	2.23E − 05
XS2-Centre-30 cm	5.0E − 08	2.18E − 05
XS2-Centre-100 cm	2.5E − 07	3.36E − 07
XS2-Right-30 cm	3.4E − 08	1.02E − 07
XS3-Centre-30 cm	6.6E − 10	NS
XS3-Centre-100 cm	1.0E − 09	NS
Upgradient	1.1E − 09	NS
Downgradient	1.0E − 09	NS

ND—No data collected because of equipment malfunction.
NS—Not sampled during specified series of tests.

(L), and T_o is the time required for 63% recovery of the water depth (T).

RESULTS

Site characteristics

Soil at the site typically consisted of an organic surface layer in the swale up to ~0.2 m thick, a substantial clay layer ~0.5–1.0 m thick, and gravel mixed with sand and finer sediment (may be an abandoned streambed or paleochannel) starting ~0.7–1.0 m deep (Figure 2). Overall, K of soils was low. Soils at XS1 generally had the highest K while soils near XS3 generally had the lowest (Table II). Piezometers 100 cm BGS along the centreline (in the gravel layer) showed higher K than those at 30 cm BGS (in the clay layer). The only exception is XS1-Centre-30 cm, which also showed high K relative to other piezometers. This is likely because of the presence of a preferential flow path (discussed below).

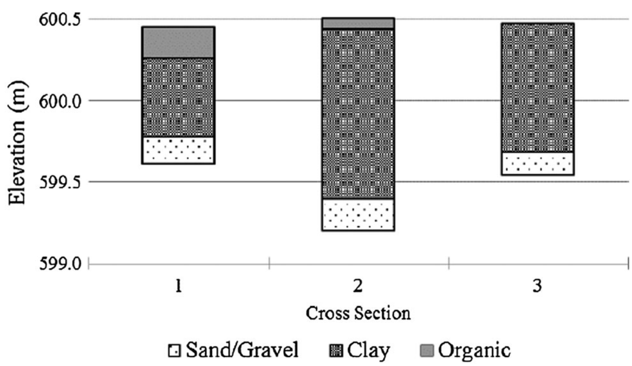

Figure 2. Soil cores extracted along site centreline

K increased at all piezometers between the 2013 and 2014 rising head tests (Table II). The increase at most piezometers was an order of magnitude or less. In two piezometers (XS2-Left-30 cm and XS2-Centre-30 cm) the increase was between 2 ½ and 3 ½ orders of magnitude. The increase at those two piezometers is dramatic, but we are confident that it is real rather than a methodological error such as short circuiting down the piezometer borehole, because the temperature and conductance of the water in the piezometer during the rising head tests did not approach that of surface water above.

Visual assessments were utilized to qualitatively track seasonal changes in vegetation density (Figure 3). Vegetation densities within the water column were minimal during the Spring flood when most herbaceous plant matter from the previous year had already partially decayed and been compacted by snow from the previous winter. Between the Spring and Early Summer floods, there was tremendous growth in herbaceous vegetation resulting in grass heights of greater than 1 m during both summer floods, particularly along the swale centreline. High vegetation persisted at least until the Late Summer flood, and then started its annual senesence. By the Fall flood in November, many stems had collapsed partway back to the ground, thereby further increasing the density of vegetation in the surface water column.

Background data collected throughout the year

Surface water and groundwater levels were generally lowest during late summer and fall (September through December 2013) because of decreased precipitation during this period and higher evapotranspiration in late summer (Figure 4, Table I). There was a corresponding reduction in head gradient between the hillslope (Upgradient) and riparian groundwater (Downgradient) during the fall, but never a reversal. At XS1-Centre, water levels in groundwater were closely related to those in surface water throughout the year. Groundwater levels at XS1 therefore appear to be affected more by surface water conditions than by larger scale seasonally-driven horizontal head gradients in groundwater. Similarly, water elevations at XS2-Centre-100 cm were often either greater or less than both the Upgradient and Downgradient piezometers rather than being at an elevation between the two as would be expected if water elevations were driven by upgradient groundwater contributions. The paleochannel in which the deep piezometers are likely screened may have accelerated draining of the floodplain. These parts of the swale along the flow centreline (e.g. XS1-Centre, XS2-Centre) therefore appear to be more influenced by vertical infiltration than lateral inflow. Seasonal variations in groundwater elevation were interrupted by both the

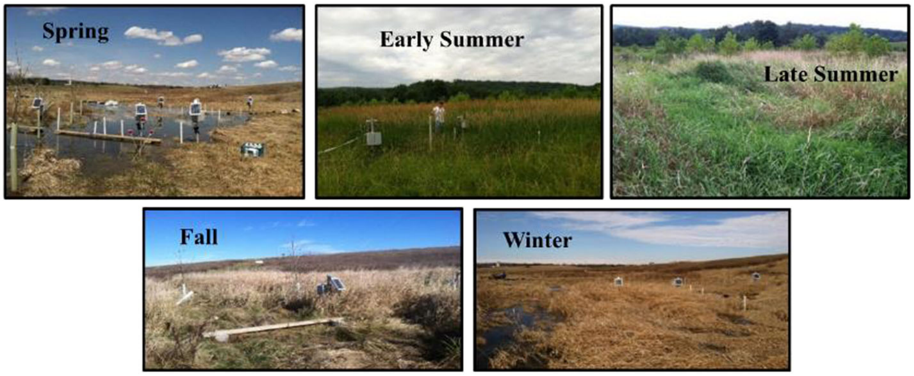

Figure 3. Seasonal variation in floodplain vegetation

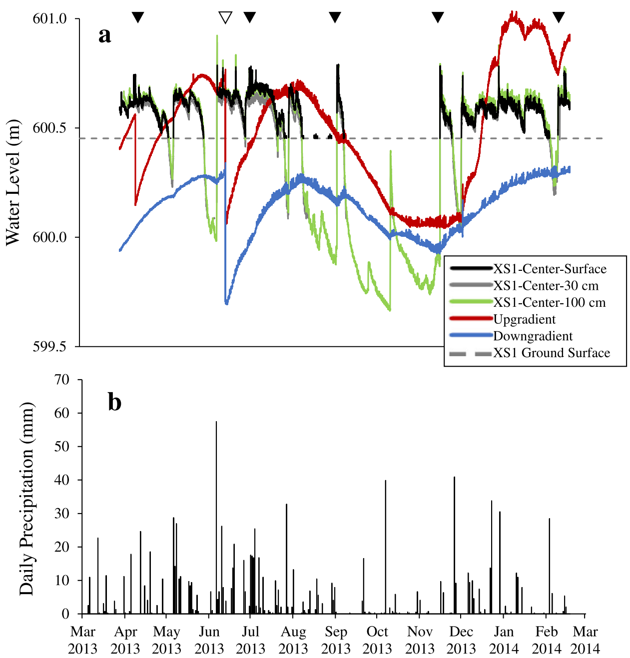

Figure 4. (a) Background surface water and groundwater levels measured at Upgradient and Downgradient piezometers (100 cm BGS), XS1-Centre-Surface, XS1-Centre-30 cm (piezometer 30 cm BGS), and XS1-Centre-100 cm (piezometer 100 cm BGS) and (b) precipitation at study site from March 2013 through March 2014. Solid inverted triangles indicate experimental flood events, and the hollow inverted triangle indicates when a rising head test was performed. BGS = (depth) below ground surface

experimental floods (Figure 4, solid inverted triangles) and the rising head tests (Figure 4, open inverted triangle), with the largest examples of the former occurring at XS1 and the largest examples of the latter occurring at the Upgradient/Downgradient piezometers.

Moisture content followed seasonal trends similar to water levels, with a drier period during late summer and fall 2013 (Figure 5). Drying occurred less along the floodplain centreline than at the Left and Right locations, was less at 10 cm depth than at 5 cm depth, and was also less at XS1-Centre than at XS2-Centre or XS3-Centre because XS1-Centre was topographically lower and therefore inundated for longer periods. Soil moisture content and groundwater levels increased quickly after each rainfall event (Figures 4 and 5).

Data collected during experimental floods

Site water balance. Inflow to floodplain surface water from the pump was approximately equal to the surface water outflow through the flume toward the end of each 3-h pumping period (Figure 6). This occurred when outflow through the flume peaked/plateaued indicating approximate steady state surface water hydraulics. Water losses because of leakage of flood water around the flume were therefore minor relative to surface flow through the site. The greatest discrepancy (~1.8 L s^{-1}) between inflow and steady state outflow occurred during the second day of the Fall flood, possibly because of inaccuracy of the two flow meters or unaccounted surface water leaving the site.

The flood wave arrival times at the flume ($T_{surface}$) were either the same or earlier for the second day flood relative to the first, with the largest differences for Late Summer and Fall when antecedent conditions were driest and the smallest difference for Spring when antecedent conditions were very wet (Figure 6, 7a). The percent of total flood water storage relative to water pumped ($V_{total\ storage}$/V_{pumped}) for the first day of flooding was greatest during the Late Summer and Fall flood when antecedent soil moisture and water levels were lowest (Figure 7b).

The percentage of drained floodwater relative to water pumped ($V_{drained}$/V_{pumped}) generally increased between the Spring and Fall experimental floods (Figure 7c). $V_{drained}$ is a surrogate for total surface water storage because floodplain topography is likely constant for a given flow rate as used in this study (Table I). As the floodplain vegetation density increased from Spring to Summer (Figure 3), the average floodplain roughness (i.e. Manning's n) increased. Because water in the swale is flowing, increased roughness should increase surface

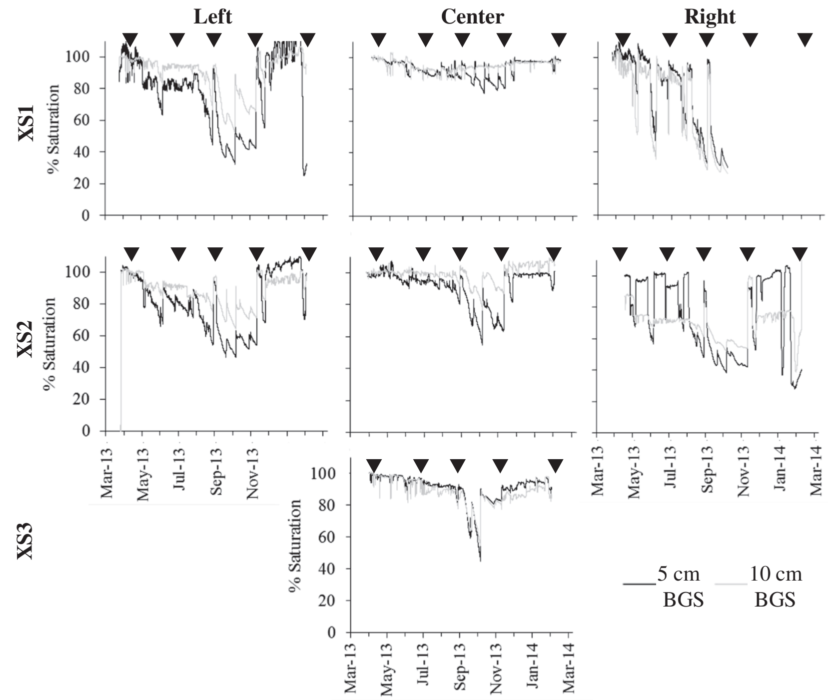

Figure 5. Background soil moisture content throughout floodplain at 5-cm and 10-cm BGS. Data were not collected from XS1-Right for the second half of the year because of malfunction of the data logger being used. Inverted triangles indicate start of experimental flood events. BGS = (depth) below ground surface

water depths and decrease surface water velocities, assuming an approximately constant inflow rate (Table I).

Surface water and groundwater hydraulics. Surface water levels showed clear increases and subsequent decreases during each flood event (Figure 8). Three types of pressure response were observed in the subsurface: an immediate response (Figure 8a), a delayed and muted response (Figure 8b), and no response (Figure 8c). An increase in vertical connectivity across the floodplain surface occurred over the course of the year, as shown by an increase in the magnitude of response ($\Delta H_{subsurface}/\Delta H_{surface}$, Figure 7d) and a decrease in response time ($T_{subsurface}$) in the subsurface (Figure 7e, Table III). The latter is particularly evident when considering groups of seasons with similar antecedent moisture conditions (decrease from Spring to Early Summer to Winter for wet conditions, and from Late Summer to Fall for dry conditions).

Vertical head gradients across the floodplain surface (I_z) at XS1-Centre quickly approached neutral conditions (i.e. gradient = 0) during each of the five floods regardless of pre-flood groundwater levels (Figure 9a). By contrast, I_z at XS2-Centre often showed more pronounced losing conditions at the beginning of the floods (Figure 9b), particularly during the first day of flooding in both Late Summer and Fall where antecedent moisture conditions were drier (not shown). Finally, I_z at XS3-Centre showed strong losing conditions that heightened upon the start of pumping because of stage increases in surface water (Figure 9c). Subsurface lag times ($T_{subsurface}$) show that if Darcy flow dominated surface water–groundwater exchange at the site, the required time for surface water to reach each monitoring point would be substantial and range from 5 h to multiple years (Table III). The longest of these theoretical travel times is for the very low K values (Table III) associated with the clay layer in the absence of preferential flowpaths.

Shallow soils throughout the site were drier prior to the Late Summer and Fall floods than in other seasons (Figure 5). Substantial increases in moisture levels were therefore observed during the first day flood but not during the second (Figure 10). With drier antecedent conditions in Late Summer and Fall, wetting of the shallow soils occurred simultaneously with surface inundation (Figure 11). Furthermore, wetting at 10 cm BGS occurred simultaneously or even slightly before wetting at 5 cm BGS. This may indicate that the wetting front moved laterally above the clay layer as the floods began rather than downward from surface water.

Electrical conductance. The specific conductance (SC) patterns were fairly complex, so we focus here on responses to two main perturbations occurring during the experimental floods. The first type of perturbation is pumping of stream water onto the floodplain. The SC of

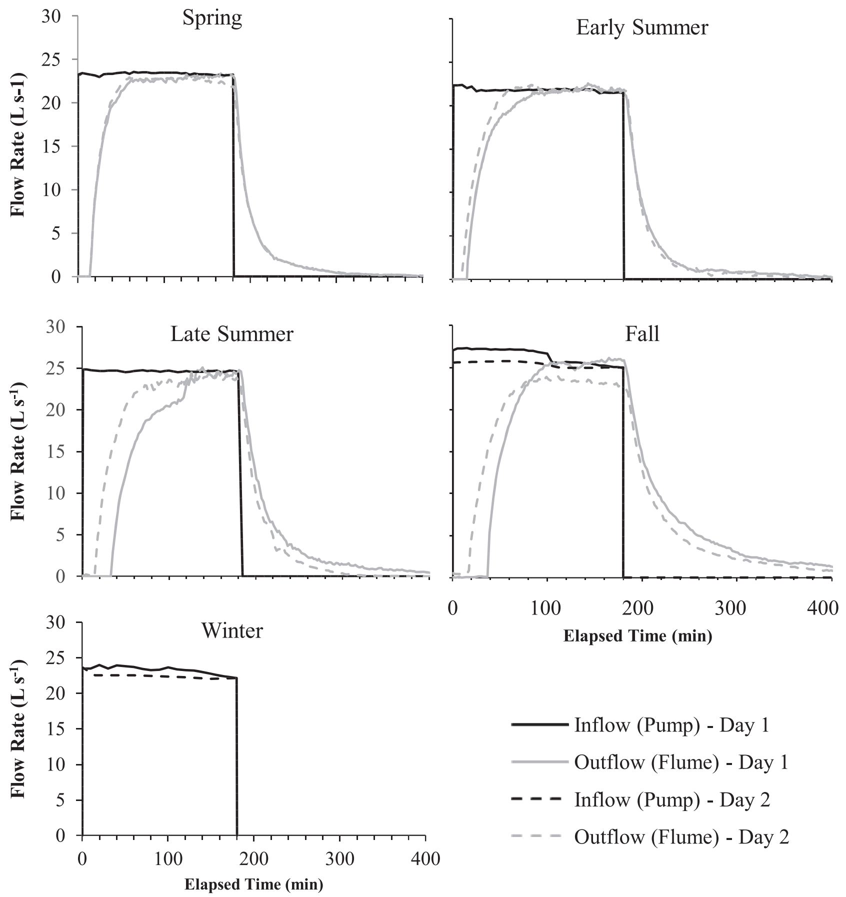

Figure 6. Inflow and outflow of surface water at flood site. Flume data were not recorded during the Winter flood because of a malfunction in the pressure sensor at that location. Day 1 and day 2 are difficult to discern where the two lines are directly atop one another (e.g. inflow for day 1 and 2 for Spring, Early Summer, and Late Summer)

water on the floodplain surface approached the SC recorded in Stroubles Creek during each flood event. Three types of groundwater SC responses were observed from the application of surface water. The first was a pulse increase (Figure 12a; 30 cm BGS) where rise and fall of groundwater SC coincided with pump on and pump off. The second type of response was a step increase in groundwater SC with no decrease after pumping ceased (Figure 12b). This type of response was most common during floods when antecedent moisture conditions were low (i.e. Late Summer and Fall). The third type of response was no SC response at all (Figure 12c). Finally, no response of groundwater SC was observed anywhere during the Winter flood.

The second type of perturbation is the salt injection pulse that occurred 120 min after start of each flood. The response in surface water was variously a spike (Figure 12c), a step (Figure 12b), or not apparent at all (Figure 12a). This variability is probably because of variability of topography and vegetation characteristics in time and space affecting surface water flowpaths, but may have been accentuated by the short duration of the spike relative to the logging frequency of the sensors. A response was never observed in groundwater because the volume of the salt tracer was relatively small.

DISCUSSION

Variation and controls on vertical connectivity across the floodplain surface

Types and spatial heterogeneity. We conceptualized four mechanisms of vertical connectivity of hydraulic or solute signals across the floodplain surface that may be occurring at our site (Figure 13). These mechanisms were derived from observations of both water level and SC in surface and subsurface water. While there is varying uncertainty associated with the occurrence of each mechanism, this conceptualization facilitates the description of observed spatial and temporal variability observed in vertical connectivity.

The first type of vertical connectivity is hydrostatic pressure propagation across the floodplain surface, where transient pressure signals from the flood wave passage in

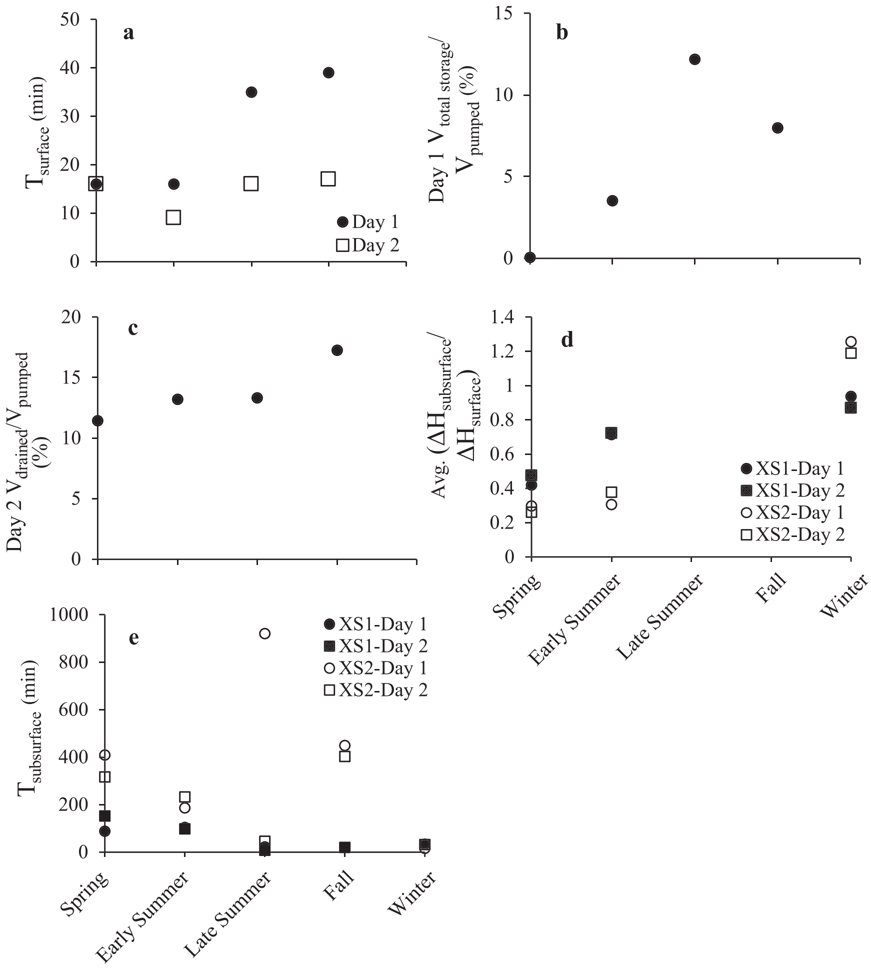

Figure 7. (a) Flood arrival time at the Parshall flume ($T_{surface}$) following beginning of each flood, (b) percent of total water applied to site that went into storage ($V_{total\ storage} / V_{pumped} \times 100$) during first day of flooding, (c) percent of total water applied to site which drained out of site following the end of each second day of flooding ($V_{drained} / V_{pumped} \times 100$), (d) change in groundwater level ($\Delta H_{subsurface}$) between pre-event conditions and peak flood-induced water level normalized to change in surface water level ($\Delta H_{surface}$) averaged across each transect for each experimental flood (Late Summer and Fall missing because conditions were dry and therefore water levels were below the piezometer screens and not measured), and (e) lag time between peak surface water level and peak groundwater level ($T_{subsurface}$) averaged across all four piezometer screens in each transect for each experimental flood (note that for Winter, XS1 and XS2 points lie directly atop one another so that the XS2 points are hard to see)

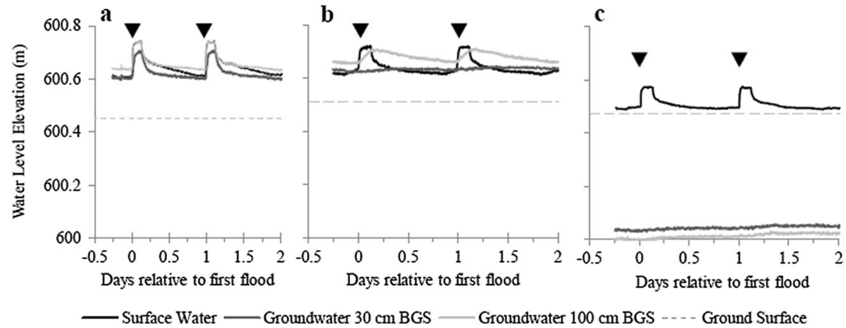

Figure 8. Example water level responses at (a) XS1-Centre, (b) XS2-Centre, and (c) XS3-Centre during Spring experimental floods. Inverted triangles indicate start of experimental flood events. BGS = (depth) below ground surface

surface water are transmitted essentially instantaneously down into the subsurface with no corresponding SC signal observed. Signals at the XS1-Centre-100 cm piezometer were consistent with this type of connectivity where pressure signals mirrored those at the surface (Figure 8a) yet there was no SC signal (e.g. Figure 12a,

Table III. Theoretical Darcy travel times (T_{Darcy}) compared to actual signal propagation times ($T_{subsurface}$)

Piezometer	T_{Darcy} (h)	$T_{subsurface}$ Spring (min)	$T_{subsurface}$ Winter (min)
XS1-Centre-30 cm	5	17	7
XS1-Centre-100 cm	12	12	3
XS2-Centre-30 cm	4	N/A	0
XS2-Centre-100 cm	566	175	30
XS3-Centre-30 cm	42 088	N/A	N/A
XS3-Centre-100 cm	69 288	N/A	N/A

T_{Darcy} is theoretical time for water to move between surface water and groundwater monitoring points because of maximum flood-induced vertical head gradients (I_{max}) at centreline piezometers calculated using Equations (3–4) compared to actual lag times ($T_{subsurface}$) calculated using the pressure data obtained from the first day of flooding. N/A indicates no flood signal was seen at that depth.

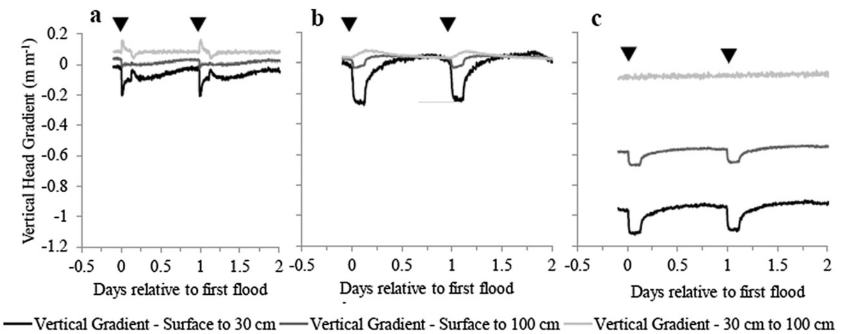

Figure 9. Example vertical head gradient responses at (a) XS1-Centre, (b) XS2-Centre, and (c) XS3-Centre during Spring experimental floods. Inverted triangles indicate start of experimental flood events. BGS = (depth) below ground surface

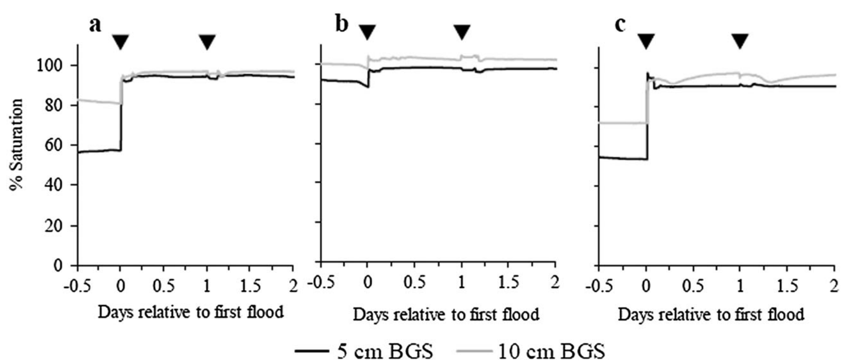

Figure 10. Example percent water saturation responses at 5 cm and 10 cm below ground surface (BGS) at (a) XS1-Centre, (b) XS2-Centre, and (c) XS3-Centre during Late Summer experimental floods. Inverted triangles indicate start of experimental flood events

100 cm). This might happen if there are a series of interconnected tortuous macropores between the surface water and the subsurface pressure sensor. In this case the pressure would be transmitted essentially instantaneously through hydrostatic means along the macropores, but the tortuous length of the macropores may be cumulatively too long to transmit SC, at least with the degree of head change that occurred in surface water. This may be analogous to pressure or kinematic waves observed in floodplains by others (Burt *et al.*, 2002; Käser *et al.*, 2009; Vidon, 2012) where the pressure signal moves rapidly from the channel into the floodplain subsurface. Yet there are important differences between the two situations given that propagation direction in one case is vertical and in the other it is horizontal. Regardless, neither of these phenomena are well understood and may be heterogeneous within small spatial scales (compare the panels in Figure 8).

A second type of vertical connectivity is bulk Darcy flow through the soil matrix (Figure 13) where viscous forces dominate (Darcy, 1856). This flow mechanism must have been ubiquitous throughout the floodplain,

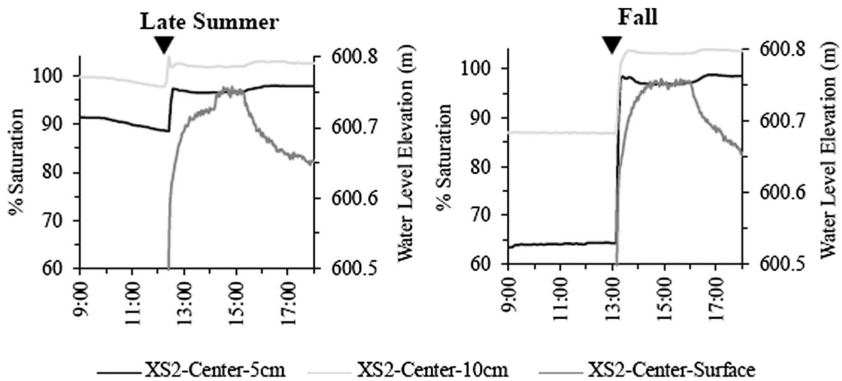

Figure 11. Surface inundation and soil moisture wetting at XS2-Centre during first day of Late Summer and Fall floods (30 August 2013 and 11 November 2013, respectively). Inverted triangles indicate start of experimental flood events. Percent saturation is presented rather than volumetric water content because porosity was spatially heterogeneous, making percent saturation more comparable among locations. This process was calibrated by setting percent saturation to 100% during periods when we know the soils were saturated for months (e.g. winter and early spring). This calibration process is not perfect, so percent saturation sometimes exceeds 100% by small amounts. This does not affect the trends that are important in our analysis and therefore does not affect our conclusions

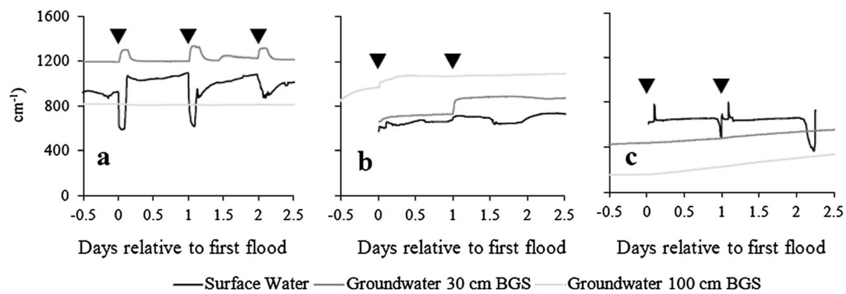

Figure 12. Example specific conductance responses in groundwater during experimental flood events including (a) pulse increase/decrease (shown is Early Summer at XS1-Centre), (b) step increase (shown is Late Summer at XS2-Centre), and (c) no response (shown is Late Summer at XS3-Centre). Inverted triangles indicate start of experimental flood events. The middle flood event in panel a (day = 1.0) experienced a piping malfunction that necessitated repeating the flood (Table I). BGS = (depth) below ground surface

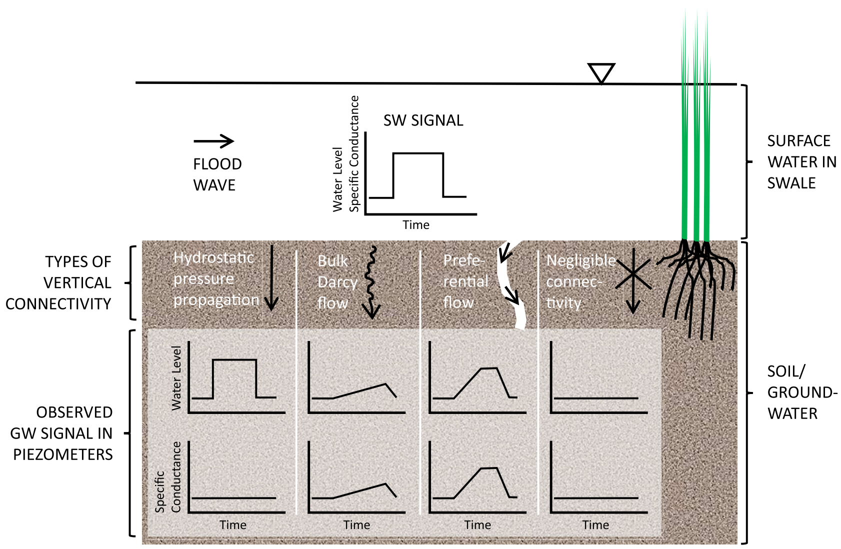

Figure 13. Potential floodplain surface water–groundwater vertical connectivity classifications. Preferential flow and Darcy flow are different mainly by degree of observed signal. Note that a pure bulk Darcy flow signal by itself was not actually observed at the piezometers. SW = surface water; GW = groundwater

occurring anywhere vertical head gradients were created by the inundation. Where soils are heterogeneous, a third type of vertical connectivity (preferential flow) occurs where water moves faster than bulk Darcy flow. Preferential flow can be either Darcy flow through regions of higher K or possibly non-Darcy flow at higher Reynolds numbers in void spaces or macropores such as those from animal burrows or root channels (Aubertin, 1971; Beasley, 1976; Beven and Germann, 1982; Menichino *et al*., 2014; Menichino and Hester, 2015). Preferential flow is likely occurring from the surface downward toward XS1-Centre-30 cm because the pressure signal at depth mirrors that at the surface (e.g. Figure 8a) but there is also rapid response of SC at depth (e.g. Figure 12a, 30 cm; Figure 14). By contrast, a mix of bulk Darcy flow and preferential flow is likely occurring to XS2-Centre-100 cm (Figure 8b). The response is delayed relative to XS1-Centre-30 cm, but based on K at XS2-Centre-100 cm and the depth to measuring point, the peak in water elevation occurs too quickly to be explained by Darcy flow alone (Table III). Preferential flow influencing XS2-Centre-100 cm was particularly apparent given the lack of signal at the intermediate location XS2-Centre-30 cm. Quantitatively distinguishing between bulk Darcy flow and preferential flow was not possible with our data set, and would require greater spatial resolution of floodplain soil structure including preferential flowpaths such as soil pipes.

Fourth, there were locations that experienced little or no vertical connectivity or SC response. This is seen at XS3-Centre-100 cm (e.g. Figures 8c, 12c, 13) and persisted through the wetter seasons (e.g. Spring, Early Summer, and Winter floods) when K of soils would typically be higher (Pirastru and Niedda, 2013), suggesting the clay layer was relatively impermeable and lacked preferential flow paths. The distinction between the second and fourth types of vertical connectivity discussed here is probably more a quantitative distinction than a qualitative distinction, in that Darcy flow is surely occurring in both cases, but in the fourth situation it has minimal effect because of the low K clay layer.

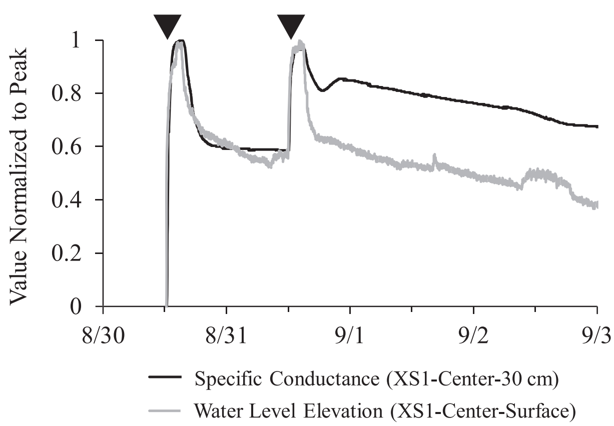

Figure 14. Water level and specific conductance normalized to peak values during Late Summer experimental flood. Inverted triangles indicate start of experimental flood events

Temporal variation. With the exception of XS3, groundwater levels during floods indicate an increase in vertical connectivity across the floodplain surface over the course of the year. This manifested as an increase in flood signal (Figure 7d) and an increase in signal propagation speed at some locations (Figure 7e, Table III). Observed patterns are consistent with an expansion of pressure propagation in most cases, with only a few piezometers indicating change in SC in the subsurface. As discussed above in the section Types and spatial heterogeneity, this could occur where interconnected tortuous macropores allow rapid pressure propagation but are cumulatively too long to transmit SC all the way to the sensor given the head change in surface water. Such increases in vertical connectivity may have been a result of soil piping. This can occur at the interface of two soils with considerably different hydraulic conductivities (*Jones*, 1971), which are present at our site. The frequency of overbank floods that we simulated exceeded those during natural storms during the year at this site. This increase in head may have accelerated the formation of PFPs through increases in pipe erosion. Furthermore, the more frequent inundation and application of nutrients in the surface water may have led to greater vegetative root structure, potentially enhancing formation of macropores (Bramley *et al*., 2003). We acknowledge that we did not directly measure increases in floodplain macroporosity, and thus this explanation for increased vertical connectivity remains a hypothesis. Future studies could verify this process through simultaneous use of soil pipe mapping techniques such as geophysical methods (Menichino *et al*., 2014) or injection of a hardening substance like latex (Abou Najm *et al*., 2010).

The increase in vertical connectivity across the floodplain surface is consistent with the concomitant increase in K. For example, one of the greatest increases in K was at XS2-Centre-30 (Table II), and at this location we saw a change from no pressure signal observed at depth to propagation of the signal to depth essentially instantaneously (Table III). The increase in vertical connectivity between the surface and subsurface in some cases was even more substantial than could be explained by such increases in K, showing increases from no propagation of signal to showing an immediate propagation of pressure signal at a variety of locations (XS1-Left, XS1-Right, XS2-Centre-30 cm, XS2-Left, XS2-Right). Therefore, new preferential flow paths may have been created in areas that were beyond the area of influence of the rising head tests we performed.

Antecedent moisture conditions also appeared to control temporal variation in subsurface response. When antecedent moisture was low during the Late Summer and Fall floods, SC at XS2-Centre-100 cm approached that of surface water (e.g. Figure 12b). Conversely, when antecedent moisture was high (i.e. Spring, Early Summer, and Winter), subsurface SC responded much less—in fact, there were no SC responses except Spring and Early Summer at XS1-Centre-30 cm. Mixing of infiltrating surface water with pre-existing groundwater may have resulted in this lack of SC signal.

Effects of seasons and antecedent moisture on floodplain storage

Changing seasons strongly affected vegetation density in the experimental flood area (Figure 3). Because of unseasonably wet conditions during the first half of summer, the Spring and Early Summer floods had essentially identical antecedent moisture conditions (i.e. saturated soils), which allows us to attribute observed changes to effects of vegetation density and/or evapotranspiration. The increase in vegetation density between these two seasons increased the floodplain roughness, which according to open channel flow theory would increase flow depths and decrease velocities, such that more surface water is stored on the floodplain and less of this water has left the system before the pump is turned off, leading to increases in $V_{drained}$ (Figure 7c). However, the Fall flood showed yet a further increase in $V_{drained}$ despite the greatest vegetation growth occurring during the Summer. The dieback and collapse of vegetation prior to the Fall flood appear to concentrate more biomass in the water column than when vegetation is upright during the summer. This may create a correspondingly greater impact on floodplain hydraulic roughness and hence $V_{drained}$ during the Fall compared to the Summer. In other words, rather than the vegetation height, the most important factor appears to be the amount of vegetation that directly impedes surface flow (Luhar and Nepf, 2013).

Vegetation conditions and $V_{drained}$ (Figures 3 and 7c) were nearly identical during the Early and Late Summer floods. This allows us to attribute the greater $T_{surface}$ and $V_{total\ storage}$ during the Late Summer flood relative to Early Summer (Figures 7ab) to decreases in antecedent soil moisture and water levels. Because $V_{total\ storage}$ increases between Early and Late Summer (Figure 7b), yet $V_{drained}$ does not change (Figure 7c), drier antecedent conditions must increase $V_{subsurface\ storage}$, and hence vertical connectivity across the floodplain surface. This increase in flood water moving to $V_{subsurface\ storage}$ then slows movement of surface water across the floodplain surface, increasing $T_{surface}$ (Figure 7a). This increase in $V_{subsurface\ storage}$ and hence vertical connectivity may then lead to greater potential for biogeochemical processing and pollutant reactions.

Applied implications of heterogeneous vertical connectivity

Our data suggest that multiple flow mechanisms can occur within small areas of floodplains. It therefore seems unreasonable to assume that the subsurface of floodplains, as well as surface water–groundwater exchange mechanisms across floodplain surfaces, are generally homogeneous (Bates *et al*., 2000; Krause *et al*., 2007). This makes field assessment and also numerical modelling of floodplain groundwater flow and surface water–groundwater interactions in floodplains more difficult. In such an environment, point measurements like those using piezometers may be less useful than distributed methods like electrical resistivity or distributed temperature sensing (Selker *et al*., 2006; Menichino *et al*., 2014).

Nevertheless, such heterogeneity may offer benefits. Preferential flow can enhance transport of flood water into the subsurface depending on preferential flowpath connectivity (Nieber, 2000). For example, preferential flow of flood water back to the surface or channel reduces contact with floodplain sediments. Yet preferential flow that bypasses restrictive (low K) layers to access to deeper soils could increase contact with roots and redox conditions conducive for biogeochemical reactions (Fuchs *et al*., 2009; Heeren *et al*., 2010). This is particularly relevant at sites such as ours where the restrictive layer is extensive.

Experimental floods with higher floodplain vegetation density in the water column had greater surface storage of flood water ($V_{drained}$) (Figure 7c) and therefore likely greater residence time of flood water given similar pumping rates. During over bank events, this would allow for increased sediment deposition (Kronvang *et al*., 2007) and contact with terrestrial plants that can increase nutrient removal via plant uptake (Lewandowski and Nützmann, 2010). As discussed in the section Effects of seasons and antecedent moisture on floodplain storage, antecedent moisture affected $V_{subsurface\ storage}$, with lower antecedent moisture allowing for greater infiltration across the floodplain surface and greater $V_{subsurface\ storage}$. Fully understanding the effect of these hydraulic parameters on nutrient cycling is important when determining the potential benefits stemming from floodplain reconnection (Jones *et al*., 2015).

Limitations of study

When visually comparing vegetation density at the time of instrument installation (March, 2013) to the density at the end of the experimental year (March, 2014), it is clear that the flood events themselves altered vegetation growth. In addition to increasing inundation relative to natural conditions, nutrients were added during each flood to quantify biogeochemical parameters as part of a separate study (Jones *et al*., 2015). This likely accelerated vegetation growth in the flooded area. In addition, as discussed earlier, the frequency of simulated overbank floods exceeded that of natural floods in this system, possibly increasing preferential flow.

Our floods did not fully replicate conditions during natural overbank events, in that the channel was not at flood stage. In a natural flood, groundwater levels near the stream would increase as channel stage approaches overbank elevation (Burt *et al*., 2002; Jung *et al*., 2004; Sawyer *et al*., 2009). In other words, in natural floods, channel water would enter floodplain soils and groundwater both vertically across the floodplain surface (vertical connectivity) and horizontally across the channel banks (bank storage). While both processes can be important, vertical connectivity was the primary process in our study, with negligible effects of lateral connectivity across channel banks. This assertion is based on the fact that background data collected during the interim between experimental floods (Figure 4) show that, even at our closest piezometer to the channel ('Downgradient'), the effects of natural storm events on groundwater levels are generally not discernible, and in the few cases where a water level rise can be seen, it was only a few centimetres. The greater distance of the floodplain swale from the channel indicates that the effects of bank storage there must be even less. Hence, bank storage and lateral connectivity between the channel and floodplain can be neglected in our analysis.

A more realistic flood experiment that included a rise in channel stage could affect hydraulic gradients across the channel banks. Such channel–floodplain gradients could be quite strong, and could have a substantial effect on the floodplain groundwater flow field, depending on their strength relative to the downvalley gradient. The relative strengths of these gradients could also vary in time on storm event and annual scales. As discussed earlier, such channel–floodplain gradients were small in our experiments, but may be more important at other sites, affecting vertical head gradients. The degree of this effect would depend on distance from the channel, hydraulic conductivities, and magnitude of channel stage rise. Nevertheless, the diversity, spatial heterogeneity, and long-term temporal trends of vertical connectivity mechanisms that are the focus of our study likely would remain unchanged.

While our study does not capture the high channel stages typical of natural flooding, we emphasize the value of experimental studies of this type. It would be impossible to conduct our experiments during actual flood events. Yet our experiments address the issues that have plagued prior work on floodplains, where flow rate across the floodplain varied simultaneously with other controlling variables such as season. Our approach does not suffer from these issues, and therefore complements prior studies to build the body of knowledge regarding floodplain hydraulic response.

CONCLUSIONS

In our experimental overbank floods, the effects of seasons and moisture were primarily on storage of floodwater within the floodplain. Seasonal variation affected floodplain vegetation which primarily affected surface storage volume in seasons where vegetation added roughness elements in the surface water column. Although vegetation growth was greatest during the summer, the matting down of this vegetation during the fall resulted in the greatest surface water volume at that time.

By comparison, antecedent moisture primarily affected transfer of water vertically across the floodplain surface and therefore subsurface storage, which in turn led to decreased flood wave propagation speed. Greater increases in soil moisture and groundwater levels over the course of flood events, as well as associated solute migration into the subsurface, were observed when antecedent moisture conditions were low. At the same time, because this subsurface storage of flood water increased, the fraction of applied flood water stored cumulatively in both the surface and subsurface also increased. As stream stage receded following the flood event, the stored water remained present within the floodplain with potential for pollutant reactions. Greater topographic complexity and vegetation density in floodplain reconnection projects will allow for increased flood water retention and therefore greater potential for pollutant removal. These effects of season and antecedent moisture are intuitive and likely occur at many sites with overbank flooding.

In contrast, seasons did not appear to affect vertical surface water–groundwater connectivity across the floodplain surface as measured by patterns of hydraulic and SC response in the subsurface. These patterns were highly heterogeneous in space, with four types potentially occurring at the site, including hydrostatic pressure propagation, bulk Darcy groundwater flow, preferential groundwater flow, and a lack of connectivity in some locations. The relative dominance of these types of connectivity likely varies among sites, but the range of types of connectivity and their spatial heterogeneity may be common.

Rather than depending on season or moisture variations, there was a consistent increase in vertical connectivity across the floodplain surface over the course of the year in many parts of the floodplain. This indicates that the act of flooding itself appears to increase surface water–groundwater exchange across the floodplain surface, perhaps through the expansion of preferential flowpaths. The significance of preferential flow for water quality is likely variable depending on whether such flow increases access of flood water to deeper soil strata where reactions may occur or alternatively bypasses otherwise reactive sediments to quickly return flow to the channel. This hydraulic complexity suggests that distributed field methods which give a more holistic picture of groundwater movement may be helpful.

ACKNOWLEDGEMENTS

The authors thank the National Science Foundation (ENG-CBET-1066817) and the Institute for Critical Technology and Applied Science at Virginia Tech for support. Opinions expressed here are those of the authors and not necessarily those of the NSF. The authors thank Cully Hession and Laura Lehmann for access to the VT BSE StREAM Lab and the many volunteers for their field assistance. The authors thank several anonymous reviewers for helpful comments that substantially improved this manuscript.

REFERENCES

Abou Najm MR, Jabro JD, Iversen WM, Mohtar RH, Evans RG. 2010. New method for the characterization of three-dimensional preferential flow paths in the field. *Water Resources Research* **46**: W02503.

Amoros C, Bornette G. 2002. Connectivity and biocomplexity in waterbodies of riverine floodplains. *Freshwater Biology* **47**: 761–776.

Andersen HE. 2004. Hydrology and nitrogen balance of a seasonally inundated Danish floodplain wetland. *Hydrological Processes* **18**: 415–434.

Arshad M, Lowery B, Grossman B. 1996. Physical tests for monitoring soil quality. In *Methods for assessing soil quality*. Doran JW, Jones AJ, (Eds). Soil Science Society of America, Madison, WI. p 123–141.

Aubertin, GM. 1971. Nature and extent of macropores in forest soils and their influence on subsurface water movement. Northeastern Forest Experiment Station.

Bates PD, Stewart MD, Desitter A, Anderson MG, Renaud JP, Smith JA. 2000. Numerical simulation of floodplain hydrology. *Water Resources Research* **36**: 2517–2529.

Beasley RS. 1976. Contribution of subsurface flow from the upper slopes of forested watersheds to channel flow. *Soil Science Society of America Journal* **40**: 955–957.

Bernhardt ES, Palmer MA, Allan JD, Alexander G, Barnas K, Brooks S, Carr J, Clayton S, Dahm C, Follstad-Shah J, Galat D, Gloss S, Goodwin P, Hart D, Hassett B, Jenkinson R, Katz S, Kondolf GM, Lake PS, Lave R, Meyer JL, O'Donnell TK, Pagano L, Powell B, Sudduth E. 2005. Ecology—synthesizing US river restoration efforts. *Science* **308**: 636–637.

Beven K, Germann P. 1982. Macropores and water flow in soils. *Water Resources Research* **18**: 1311–1325.

Boon PJ. 1998. River restoration in five dimensions. *Aquatic Conservation: Marine and Freshwater Ecosystems* **8**: 257–264.

Booth DB. 1990. Stream-channel incision following drainage-basin urbanization. *Journal of the American Water Resources Association* **26**: 407–417.

Bramley H, Hutson J, Tyerman SD. 2003. Floodwater infiltration through root channels on a sodic clay floodplain and the influence on a local tree species Eucalyptus largiflorens. *Plant and Soil* **253**: 275–286.

Bukaveckas PA. 2007. Effects of channel restoration on water velocity, transient storage, and nutrient uptake in a channelized stream. *Environmental Science & Technology* **41**: 1570–1576.

Burt TP, Bates PD, Stewart MD, Claxton AJ, Anderson MG, Price DA. 2002. Water table fluctuations within the floodplain of the River Severn, England. *Journal of Hydrology* **262**: 1–20.

Craig LS, Palmer MA, Richardson DC, Filoso S, Bernhardt ES, Bledsoe BP, Doyle MW, Groffman PM, Hassett BA, Kaushal SS, Mayer PM, Smith SM, Wilcock PR. 2008. Stream restoration strategies for reducing river nitrogen loads. *Frontiers in Ecology and the Environment* **6**: 529–538.

Dahan O, Tatarsky B, Enzel Y, Kulls C, Seely M, Benito G. 2008. Dynamics of flood water infiltration and ground water recharge in hyperarid desert. *Ground Water* **46**: 450–461.

Darcy H. 1856. *Les Fontaines Publiques de la Ville de Dijon*. Dalmont: Paris. 647 p. & atlas.

Doble, RC, Crosbie RS, Smerdon BD. 2011a. Aquifer recharge from overbank floods. In *Conceptual and modelling studies of integrated groundwater, surface water and ecological systems*, (Proceedings of Symposium H01 held during IUGG2011 in Melbourne, Australia, July 2011) (IAHS Publ. 345, 2011). Abesser C, Nutzmann G, Hill MC (eds). IAHS. Pages 169–174.

Doble, RC, Crosbie RS, Smerdon BD, Peeters L, Chan F, Marinova D, Andersson RS. 2011b. Examining the controls on overbank flood recharge for improved estimates of national water accounting. 19th International Congress on Modelling and Simulation (MODSIM), Perth, Australia, December 12-16, 2011.

Doble RC, Crosbie RS, Smerdon BD, Peeters L, Cook FJ. 2012. Groundwater recharge from overbank floods. *Water Resources Research* **48**: W09522.

Doll BA, Wise-Frederick DE, Buckner CM, Wilkerson SD, Harman WA, Smith RE, Spooner J. 2002. Hydraulic geometry relationships for urban streams throughout the piedmont of North Carolina1. *Journal of the American Water Resources Association* **38**: 641–651.

Fox GA, Wilson GV, Periketi RK, Cullum RF. 2006. Sediment transport model for seepage erosion of streambank sediment. *Journal of Hydrologic Engineering* **11**: 603–611.

Fuchs JW, Fox GA, Storm DE, Penn CJ, Brown GO. 2009. Subsurface transport of phosphorus in riparian floodplains: influence of preferential flow paths. *Journal of Environmental Quality* **38**: 473–484.

Graf WL. 1975. The impact of suburbanization on fluvial geomorphology. *Water Resources Research* **11**: 690–692.

Harrison MD, Miller AJ, Groffman PM, Mayer PM, Kaushal SS. 2014. Hydrologic controls on nitrogen and phosphorous dynamics in relict oxbow wetlands adjacent to an urban restored stream. *Journal of the American Water Resources Association* **50**: 1365–1382.

Heeren DM, Miller RB, Fox GA, Storm DE, Halihan T, Penn CJ. 2010. Preferential flow effects on subsurface contaminant transport in alluvial floodplains. *Transactions of the ASABE* **53**: 127–136.

Heeren DM, Fox GA, Fox AK, Storm DE, Miller RB, Mittelstet AR. 2014. Divergence and flow direction as indicators of subsurface heterogeneity and stage-dependent storage in alluvial floodplains. *Hydrological Processes* **28**: 1307–1317.

Helton AM, Poole GC, Payn RA, Izurieta C, Stanford JA. 2014. Relative influences of the river channel, floodplain surface, and alluvial aquifer on simulated hydrologic residence time in a montane river floodplain. *Geomorphology* **205**: 17–26.

Hester ET, Gooseff MN. 2010. Moving beyond the banks: hyporheic restoration is fundamental to restoring ecological services and functions of streams. *Environmental Science & Technology* **44**: 1521–1525.

Hvorslev, MJ. 1951. Time lag and soil permeability in ground-water observations. U.S. Army Corps of Engineers Waterways Experiment Station Bulletin 36. Vicksburg, MS.

Jolly ID, Walker GR, Narayan KA. 1994. Floodwater recharge processes in the Chowilla anabranch system, South Australia. *Soil Research* **32**: 417–435.

Jones A. 1971. Soil piping and stream channel initiation. *Water Resources Research* **7**(3): 602–610.

Jones CN, Scott DT, Guth CR, Hester ET, Hession WC. 2015. Seasonal variation in floodplain biogeochemical processing in a restored headwater stream. *Environmental Science & Technology* **49**: 13190–13198.

Jung M, Burt TP, Bates PD. 2004. Toward a conceptual model of floodplain water table response. *Water Resources Research* **40**: W12409.

Junk WJ, Bayley PB, Sparks RE. 1989. The flood pulse concept in river–floodplain systems. *Canadian Special Publication of Fisheries and Aquatic Sciences* **106**: 110–127.

Käser DH, Binley A, Heathwaite AL, Krause S. 2009. Spatio-temporal variations of hyporheic flow in a riffle–step–pool sequence. *Hydrological Processes* **23**: 2138–2149.

Knispel S, Sartori M, Brittain JE. 2006. Egg development in the mayflies of a Swiss glacial floodplain. *Journal of the North American Benthological Society* **25**: 430–443.

Krause S, Bronstert A. 2007. The impact of groundwater–surface water interactions on the water balance of a mesoscale lowland river catchment in northeastern Germany. *Hydrological Processes* **21**: 169–184.

Krause S, Bronstert A, Zehe E. 2007. Groundwater–surface water interactions in a North German lowland floodplain—implications for the river discharge dynamics and riparian water balance. *Journal of Hydrology* **347**: 404–417.

Kronvang B, Andersen IK, Hoffmann CC, Pedersen ML, Ovesen NB, Andersen HE. 2007. Water exchange and deposition of sediment and phosphorus during inundation of natural and restored lowland floodplains. *Water, Air, and Soil Pollution* **181**: 115–121.

Landers J. 2010. Entering the mainstream. *Civil Engineering* **80**: 58–69.

Landon MK, Rus DL, Harvey FE. 2001. Comparison of instream methods for measuring hydraulic conductivity in sandy streambeds. *Ground Water* **39**: 870–885.

Lane EW. 1955. Design of stable channels. *Transactions of the American Society of Civil Engineers* **120**: 1234–1260.

Langhans SD, Tockner K. 2006. The role of timing, duration, and frequency of inundation in controlling leaf litter decomposition in a river–floodplain ecosystem (Tagliamento, northeastern Italy). *Oecologia* **147**: 501–509.

Leopold, LB. 1968. Hydrology for urban land planning: a guidebook on the hydrologic effects of urban land use.

Lerner DN. 2002. Identifying and quantifying urban recharge: a review. *Hydrogeology Journal* **10**: 143–152.

Lewandowski J, Nützmann G. 2010. Nutrient retention and release in a floodplain's aquifer and in the hyporheic zone of a lowland river. *Ecological Engineering* **36**: 1156–1166.

Luhar M, Nepf HM. 2013. From the blade scale to the reach scale: a characterization of aquatic vegetative drag. *Advances in Water Resources* **51**: 305–316.

Menichino GT, Hester ET. 2015. The effect of macropores on bi-directional hydrologic exchange between a stream channel and riparian groundwater. *Journal of Hydrology* **529**: 830–842.

Menichino GT, Ward AS, Hester ET. 2014. Macropores as preferential flow paths in meander bends. *Hydrological Processes* **28**: 482–495.

Mertes LAK. 1997. Documentation and significance of the perirheic zone on inundated floodplains. *Water Resources Research* **33**: 1749–1762.

Nieber, JL. 2000. The relation of preferential flow to water quality, and its theoretical and experimental quantification. Preferential Flow: Water Movement and Chemical Transport in the Environment. 2nd International Symposium on Preferential Flow. Honolulu, HI. January 3–5, 2001.1-10.

O'Driscoll M, Clinton S, Jefferson A, Manda A, McMillan S. 2010. Urbanization effects on watershed hydrology and in-stream processes in the southern United States. *Water* **2**: 605–648.

Pinder GF, Sauer SP. 1971. Numerical simulation of flood wave modification due to bank storage effects. *Water Resources Research* **7**: 63–70.

Pirastru M, Niedda M. 2013. Evaluation of the soil water balance in an alluvial flood plain with a shallow groundwater table. *Hydrological Sciences Journal* **58**: 898–911.

Poff NL, Allan JD, Bain MB, Karr JR, Prestegaard KL, Richter BD, Sparks RE, Stromberg JC. 1997. The natural flow regime. *Bioscience* **47**(11): 769–784.

Poole GC, Stanford JA, Frissell CA, Running SW. 2002. Three-dimensional mapping of geomorphic controls on flood-plain hydrology and connectivity from aerial photos. *Geomorphology* **48**: 329–347.

Pringle C. 2003. What is hydrologic connectivity and why is it ecologically important? *Hydrological Processes* **17**: 2685–2689.

Sawyer AH, Cardenas MB, Bomar A, Mackey M. 2009. Impact of dam operations on hyporheic exchange in the riparian zone of a regulated river. *Hydrological Processes* **23**: 2129–2137.

Selker JS, Thevenaz L, Huwald H, Mallet A, Luxemburg W, Van De Giesen N, Stejskal M, Zeman J, Westhoff M, Parlange MB. 2006. Distributed fiber optic temperature sensing for hydrologic systems. *Water Resources Research* **42**: W12202.

Simon, A, Bennett SJ, Castro JM (eds). 2011. *Stream restoration in dynamic fluvial systems: scientific approaches, analyses, and tools*. First edition. American Geophysical Union (Geopress): Washington, DC.

Singh VP. 2002. Is hydrology kinematic? *Hydrological Processes* **16**: 667–716.

Stanford JA, Ward JV. 1993. An ecosystem perspective of alluvial rivers: connectivity and the hyporheic corridor. *Journal of the North American Benthological Society* **12**(1): 48–60.

Thien SJ. 1979. A flow diagram for teaching texture-by-feel analysis. *Journal of Agronomic Education* **8**: 54–55.

Tockner K, Malard F, Ward JV. 2000. An extension of the flood pulse concept. *Hydrological Processes* **14**: 2861–2883.

Vidon P. 2012. Towards a better understanding of riparian zone water table response to precipitation: surface water infiltration, hillslope contribution or pressure wave processes? *Hydrological Processes* **26**: 3207–3215.

Walter RC, Merritts DJ. 2008. Natural streams and the legacy of water-powered mills. *Science* **319**: 299–304.

Ward JV. 1997. An expansive perspective of riverine landscapes: pattern and process across scales. *GAIA-Ecological Perspectives for Science and Society* **6**: 52–60.

Welch C, Cook PG, Harrington GA, Robinson NI. 2013. Propagation of solutes and pressure into aquifers following river stage rise. *Water Resources Research* **49**: 5246–5259.

Wohl E, Angermeier PL, Bledsoe B, Kondolf GM, MacDonnell L, Merritt DM, Palmer MA, Poff NL, Tarboton D. 2005. River restoration. *Water Resources Research* **41**: W10301.

